CrossMark click for updates

Epitaxial *c*-axis oriented $BaTiO_3$ thin films on $SrTiO_3$-buffered Si(001) by atomic layer deposition

Thong Q. Ngo,[1] Agham B. Posadas,[2] Martin D. McDaniel,[1] Chengqing Hu,[3] John Bruley,[4] Edward T. Yu,[3] Alexander A. Demkov,[2] and John G. Ekerdt[1,a)]
[1]*Department of Chemical Engineering, The University of Texas at Austin, Austin, Texas 78712, USA*
[2]*Department of Physics, The University of Texas at Austin, Austin, Texas 78712, USA*
[3]*Department of Electrical Engineering, The University of Texas at Austin, Austin, Texas 78712, USA*
[4]*IBM Research Division, Yorktown Heights, New York 10593, USA*

(Received 20 January 2014; accepted 16 February 2014; published online 27 February 2014)

Atomic layer deposition (ALD) of epitaxial *c*-axis oriented $BaTiO_3$ (BTO) on Si(001) using a thin (1.6 nm) buffer layer of $SrTiO_3$ (STO) grown by molecular beam epitaxy is reported. The ALD growth of crystalline BTO films at 225 °C used barium bis(triisopropylcyclopentadienyl), titanium tetraisopropoxide, and water as co-reactants. X-ray diffraction (XRD) reveals a high degree of crystallinity and *c*-axis orientation of as-deposited BTO films. Crystallinity is improved after vacuum annealing at 600 °C. Two-dimensional XRD confirms the tetragonal structure and orientation of 7–20-nm thick films. The effect of the annealing process on the BTO structure is discussed. A clean STO/Si interface is found using *in-situ* X-ray photoelectron spectroscopy and confirmed by cross-sectional scanning transmission electron microscopy. The capacitance-voltage characteristics of 7–20 nm-thick BTO films are examined and show an effective dielectric constant of ~660 for the heterostructure. © *2014 AIP Publishing LLC*. [http://dx.doi.org/10.1063/1.4867469]

The ability to grow $SrTiO_3$ (STO) epitaxially on Sr-passivated Si(001) using molecular beam epitaxy (MBE)[1] has opened up a pathway to integrate functional oxides onto silicon for the next generation of photonic and electronic devices. Over the years, a variety of functional perovskite oxides including $BaTiO_3$ (BTO) have been integrated on Si through this approach.[2–9] Ferroelectric BTO has several advantages for non-volatile ferroelectric memory applications compared to other candidates (e.g., $PbZrTiO_3$ and $SrBi_2Ta_2O_5$) particularly due to its non-toxic elements, better compatibility with integrated circuit fabrication, and lower fatigue effects.[6,9–13] Ferroelectricity is fundamentally associated with the BTO structural phase transition at the Curie temperature (T_C = 120 °C); above T_C, BTO is a paraelectric cubic perovskite ($a_{BTO(c)} = 4.005$ Å) and below T_C, it is a tetragonal ferroelectric ($a_{BTO(t)} = 3.992$ Å and $c_{BTO(t)} = 4.036$ Å) with a spontaneous polarization along the *c*-axis.[6]

The effort to integrate BTO directly on Si(001) is challenging due to the large lattice mismatch between BTO and Si (4.0% and 4.4% below and above T_C, respectively) and the reaction of Si with oxygen to form an amorphous layer that inhibits epitaxial growth. The idea of employing crystalline STO as a buffer layer to integrate BTO on Si has been demonstrated by using MBE.[6,9,11,14,15] However, MBE growth is performed at relatively high temperatures and in the presence of oxygen, leading to the formation of a significant amorphous SiO_x layer at the STO/Si interface.[12,16] The formation of this SiO_x layer may be undesirable in applications because it is in series with the perovskite films. Moreover, the mismatch between the thermal expansion coefficients of BTO/STO and Si tends to favor a polar axis lying in-plane rather than out-of-plane as the stacks are cooled down.[14,17]

It has recently been proposed that the incorporation of a ferroelectric as a gate oxide could decrease the subthreshold slope below the intrinsic thermodynamic limit of 60 mV dec^{-1} at room temperature in metal-oxide-semiconductor field effect transistors,[18] enabling even lower voltage operation of electronic devices. The moderate Curie temperature of BTO may be an advantage in this case as reported by a recent proof-of-concept demonstration of negative capacitance in $Pb(Zr_{0.2}Ti_{0.8})O_3/SrTiO_3$ metal-insulator-metal heterostructures.[19] The epitaxial growth of tetragonal BTO on Si with out-of-plane polarization in a metal-ferroelectric-semiconductor stack has been reported by a limited number of groups[6,11,14,15] and without a metallic contact by our group.[9] In this Letter, we report a low temperature chemical means of growing *c*-axis oriented BTO films with thicknesses ranging from 7–20 nm on thin (1.6 nm) STO-buffered Si(001) substrates. By keeping the substrate temperature below 225 °C during the deposition process, we are able to (i) maintain a clean STO/Si interface, free from SiO_2 and (ii) practically eliminate the effects of the difference of thermal expansion coefficients on the polarization orientation. Capacitance-voltage (C-V) measurements are also performed to demonstrate the dielectric properties of atomic layer deposition (ALD)-grown epitaxial BTO.

The 1.6-nm STO templates were grown on Si(001) by MBE using the Motorola-derived process, as described in more detail elsewhere.[16,20] Reflection high energy electron diffraction (RHEED) with an electron energy of 21 keV at a glancing angle of ~3° is used to monitor in real time the crystallinity and surface morphology of the films. The STO-buffered Si(001) substrates were then transferred *in-situ* to the ALD chamber for chemical deposition of BTO. The ALD system is a custom built, hot-wall stainless steel rectangular 20-cm long chamber, with a reactor volume of 460 cm^3.[21] Ultrahigh purity argon was used as a purge/carrier

a)Electronic mail: ekerdt@che.utexas.edu

 © 2014 AIP Publishing LLC

gas. BTO films were grown using barium bis(triisopropylcyclopentadienyl), titanium tetraisopropoxide as metal sources and water as the oxidant. The Ba and Ti precursors were held at 135 and 34 °C, respectively. The substrate temperature was maintained at 225 °C, while the working pressure was maintained at 1 Torr. *In-situ* X-ray photoelectron spectroscopy (XPS) using a VG Scienta R3000 analyzer was used to determine the film composition within an error less than 5%. A single-crystal BTO substrate from MTI, where the Ba:Ti ratio was assumed to be 1:1, was used as a standard for determining the Ba:Ti ratio of ALD-grown BTO films. The Ba:Ti ratio was adjusted by changing the cycle ratio xBa:yTi. The stoichiometry of the ALD-grown BTO films reported herein was found to be 1.1:1 (Ba:Ti) using an $x = 3$, $y = 4$ cycle ratio. Each Ba or Ti unit-cycle consisted of a 2 s pulse of the Ba or Ti precursor, respectively, a 15 s purge of Ar, a 1 s dose of water, and a 15 s purge of Ar (noted as "2/15/1/15"). The BTO films were crystalline as-deposited. Films with varying Ba:Ti ratio were grown by changing the cycle ratio x:y. It was found that the Ba-rich BTO films (up to 1.4:1 Ba:Ti) were also crystalline as-deposited, while the Ti-rich BTO films (up to 0.85:1 Ba:Ti) were amorphous even after vacuum annealing.

The film thickness and the growth rate were determined by X-ray reflectivity (XRR). X-ray diffraction (XRD) was used to determine the out-of-plane lattice constants and the crystalline quality. Two dimensional XRD was also performed to determine both the in-plane and out-of-plane lattice constants of the films. XRR and XRD were performed using an X'PERT diffractometer with a sealed-tube Cu Kα radiation source. Scanning transmission electron microscopy (STEM) was also performed to confirm the crystallinity and the nature of the STO/Si interface after BTO growth. The STEM observations were carried out using an FEI TITAN instrument. The STEM samples were prepared by FIB using standard *in-situ* lift out techniques; a capping layer of e-beam deposited Pt followed by ion beam Pt is put down. The sample is then cut using a 30 kV followed by a 5 kV Ga beam. C-V characterization of capacitor structures was performed using a Keithley 590 Analyzer interfaced to a Keithley 4200 Semiconductor Characterization System. Ti/Au top contacts (10–200 μm radius) were fabricated using photolithography, metallization via e-beam evaporation, and lift-off. For the bottom contact, the backside of Si substrates was scraped with a scalpel and placed on a copper block using a layer of In-Ga eutectic alloy in between. The bias was applied to the gold electrode, while the copper block was grounded.

The growth of BTO on Si with a native oxide was first performed to determine the effect of varying the cycle ratio on stoichiometry. Near stoichiometric 1.1:1 Ba:Ti composition was established using ALD cycle conditions of {Ba: 2/15/1/15 × 1, Ti: 2/15/1/15 × 1, Ba: 2/15/1/15 × 1, Ti: 2/15/1/15 × 1, Ba: 2/15/1/15 × 1, and Ti: 2/15/1/15 × 2} × number of ALD super-cycles. These BTO films were amorphous. The same ALD cycle conditions were then used to grow BTO on 1.6-nm STO-buffered Si(001). The BTO samples were characterized using *in-situ* RHEED after ALD growth and throughout the annealing processes. RHEED patterns of a 7-nm BTO film as-deposited and after a 5-min vacuum anneal at 600 °C taken along the [110] azimuth of STO are shown in Figs. 1(a) and 1(b), respectively. Both images show well-defined streaks indicating the high degree of crystalline order in the ALD BTO films. Sharper streaks in Fig. 1(b) compared to those of Fig. 1(a) indicate improvement in the crystallinity of post-deposition annealed films. XRR measurements found that the growth rate of amorphous BTO is 0.6 Å/unit-cycle, while the growth rate of crystalline BTO is 0.9 Å/unit-cycle. This indicates that the crystalline surface enhances the BTO growth rate similar to what we observed with STO films grown by ALD.[22]

A thinner (3 nm) BTO film was deposited on STO-buffered Si(001) to study the STO/Si interface throughout the ALD and annealing processes using *in-situ* XPS. With the initial 1.6 nm MBE-grown STO on Si(001), a small amount of Si-O (silicate) bonding at the STO/Si interface can be observed prior to ALD growth, as shown by the red color in Fig. 1(c) with a binding energy of 102 eV. There is a negligible change in Si-O bonding after ALD growth and after vacuum annealing (Fig. 1(c)—blue and green colors), demonstrating the ability of ALD to maintain a clean STO/Si interface.

XRD was used to determine the crystalline structure of ALD-grown BTO films on STO-buffered Si(001). Figure 2(a) shows θ-2θ scan of an as-deposited 20-nm thick BTO on 1.6-nm STO-buffered Si(001). The (001) and (002) Bragg peaks from BTO are present, confirming the c-axis orientation of the BTO layer. The (002) Bragg peak position at $2\theta = 45.10°$ corresponds to an out-of-plane lattice constant of 4.018 Å ± 0.005, which is slightly bigger than the bulk value of BTO cubic structure (4.005 Å). Figure 2(b) shows a reciprocal space map around the (103) BTO Bragg peak. A two-dimensional Gaussian fit was used to find the center of the peak, which was found to be at $2\theta = 74.632°$ and $\omega = 18.472°$. This corresponds to in-plane and out-of-plane

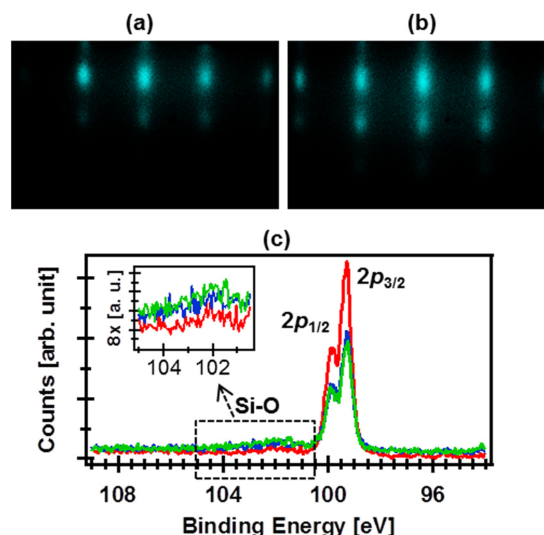

FIG. 1. (a) and (b) are RHEED patterns of a 7 nm BTO film on four-unit-cell STO-buffered Si(001) as-deposited and after 5 min vacuum anneal at 600 °C, respectively. Both images are taken along ⟨110⟩ direction of STO. (c) Si 2p XP spectra of a typical four-unit-cell STO-buffered Si(001) film (red), a 3 nm ALD BTO film on four-unit-cell STO-buffered Si(001) as-deposited (blue), and the 3 nm BTO film after a 5 min vacuum anneal at 600 °C (green). Note there is a negligible change in Si-O bonding before and after vacuum annealing and the blue and green lines are almost identical.

lattice constants of $a = 3.93 \pm 0.01$ and $c = 4.02 \pm 0.01$ Å, respectively. Different thicknesses of BTO films were grown to study the dependence of the c lattice constant on thickness. It is found that for film thickness ranging from 7 to 20 nm, the c lattice constant varies from 4.095 to 4.018 ± 0.005 Å, consistent with BTO relaxation with increasing thickness. An XRD rocking curve around the (002) Bragg peak produced a full-width at half-maximum (FWHM) of 0.91° indicating reasonable crystallinity of the as-deposited BTO films. The φ-scan indicates that there is an in-plane 45° rotation of the BTO film with respect to Si suggesting that the BTO [100] direction is parallel to the Si [110] direction.

To study the effect of post-deposition annealing on the BTO crystalline structure, the 20-nm BTO film was annealed at 600 °C for 5 min with a ramping rate of 30 °C/min. The sample was cooled below 80 °C before unloading. The (002) Bragg peak of the annealed film shifted to a position $2\theta = 45.42°$, corresponding to an out-of-plane lattice constant of 3.990 ± 0.005 Å. The (103) reciprocal space map was re-examined and showed that the lattice constants were now $a = 4.01$ and $c = 4.00 \pm 0.01$ Å. This indicates that the c-axis orientation is lost under this post-deposition annealing condition. The rocking curve around this (002) Bragg peak, however, now has a smaller FWHM value (0.74°) indicating improved crystallinity.

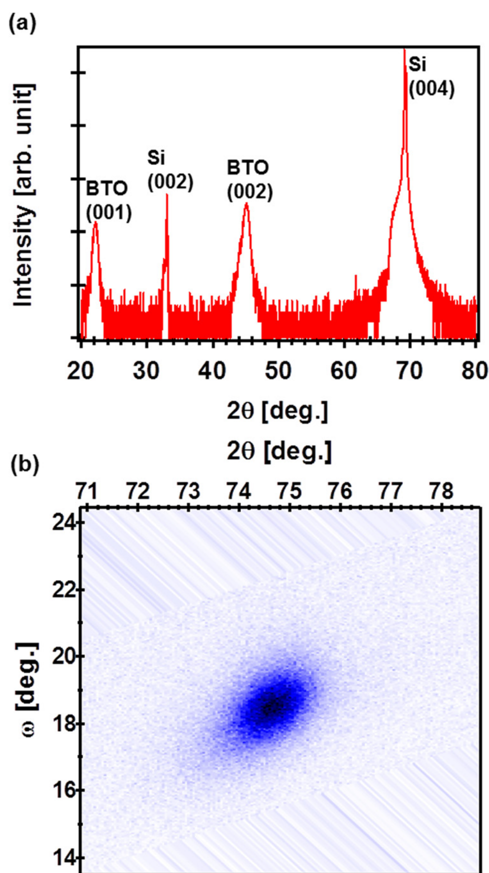

FIG. 2. (a) XRD and (b) 2D-XRD patterns of an as-deposited 20 nm ALD BTO film on four-unit-cell MBE STO on Si(001). The lattice constants of the BTO film calculated from XRD are $a = 3.93$ Å and $c = 4.02 \pm 0.01$ Å demonstrating tetragonal structure of the as-deposited BTO film.

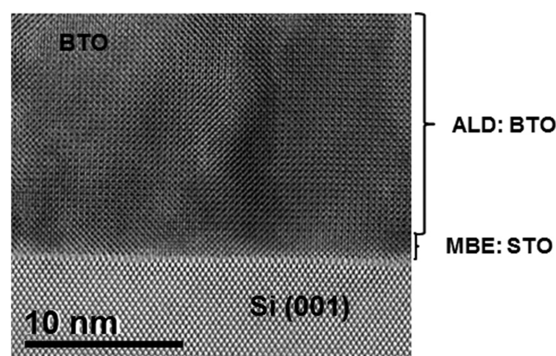

FIG. 3. STEM image of a 17 nm ALD-grown BTO film on four-unit-cell MBE-grown STO-buffered Si(001) after a 5 min vacuum anneal at 600 °C.

To study the effect caused by the difference in thermal expansion coefficients between perovskites and Si on the BTO crystalline structure, a 7-nm tetragonal BTO film ($c = 4.095 \pm 0.005$ Å) was annealed at 600 °C for 5 min with a ramping rate of 5°/min. An XRD θ-2θ scan found the out-of-plane lattice constant to be 4.045 ± 0.005 Å after annealing. This shows that by keeping ramping rate low (5°/min), we can minimize the effects of thermal expansion mismatch on the crystalline structure of tetragonal BTO.

Figure 3 shows a cross-sectional Z-contrast STEM image of a 17 nm ALD-grown BTO film on 1.6-nm STO-buffered Si(001) after 5 min vacuum anneal at 600 °C. The high degree of crystallinity of the BTO and STO layers and the abrupt STO/Si interface can be seen. No amorphous layer is observable at the interface. The image also shows that the BTO/STO interface is very sharp. The good crystalline order and very clean STO/Si interface (no amorphous layer) are consistent with RHEED, XRD, and XPS analyses.

C-V measurements at 100 kHz were performed on an 18-nm as-deposited BTO film, the results of which are shown in Fig. 4. The forward voltage sweep (−1.7 to +1.7 V, 10 mV/step, and 0.5 V/s) and reverse sweep (+1.7 to −1.7 V, 10 mV/step, and 0.5 V/s) curves are approximately identical, with no significant hysteresis observed. The ferroelectric coercive field for BTO is commonly reported to be very low with a typical value of 500 V/cm.[23,24] Even if the BTO film were ferroelectric, the low coercivity combined with the film thickness is expected to result in a hysteresis width of <10 mV. Therefore, the coercive field in the C-V data is inconclusive concerning ferroelectricity of the BTO film. The relative dielectric constant calculated from the

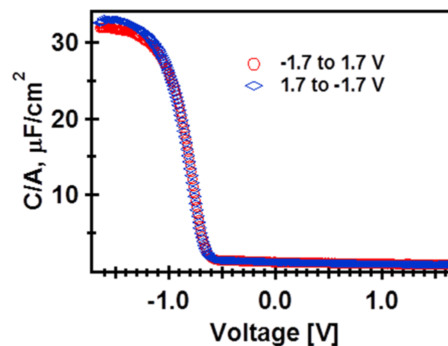

FIG. 4. C-V(at 100 kHz) characteristics of an as-deposited 18 nm BTO film on 1.6 nm STO-buffered Si(001).

accumulation side of the C-V curve was found to be ∼660, consistent with previous reports for BTO thin films.[25,26]

In conclusion, we have grown *c*-axis oriented epitaxial BTO at 225 °C using ALD on 1.6-nm STO-buffered Si(001). The BTO films have a good degree of crystallinity and no amorphous layer was observed at the STO/Si interface. A 5-min vacuum anneal at 600 °C significantly improved BTO crystallinity. Annealing using a relatively high temperature ramping rate (30 °C/min) could destroy the tetragonal structure, while annealing using a lower ramping rate (5 °C/min) is able to maintain the *c*-axis orientated tetragonal structure. The dielectric constant of the BTO/STO stack on Si was estimated to be ∼660. We expect the ALD method of growing *c*-axis oriented epitaxial BTO on STO-buffered Si(001) at low temperature to be a potential way to fabricate the negative capacitance gate oxide structure on Si with no amorphous layer between STO and Si in the near future.

This work was supported by the National Science Foundation (Award No. DMR-1207342), Office of Naval Research (Grant No. N000 14-0-1-0489), and in part (MBE growth) by the program "Understanding Charge Separation and Transfer at Interfaces in Energy Materials (EFRC: CST)," an Energy Frontier Research Center funded by the U.S. Department of Energy Office of Science, Office of Basic Energy Sciences, under Award No. DESC0001091, and the Judson S. Swearingen Regents Chair in Engineering at the University of Texas at Austin.

[1]R. A. McKee, F. J. Walker, and M. F. Chisholm, Phys. Rev. Lett. **81**, 3014 (1998).
[2]J. W. Reiner, A. M. Kolpak, Y. Segal, K. F. Garrity, S. Ismail-Beigi, C. H. Ahn, and F. J. Walker, Adv. Mater. **22**, 2919 (2010).
[3]H. Li, X. Hu, Y. Wei, Z. Yu, X. Yang, R. Droopad, A. A. Demkov, J. Erwards, K. Moore, W. Ooms, J. Kulik, and P. Fejes, J. Appl. Phys. **93**, 4521 (2003) .
[4]Z. Yu, J. Ramdani, J. A. Curless, C. D. Overgaard, J. M. Finder, R. Droopad, K. W. Eisenbeiser, J. A. Hallmark, W. J. Ooms, and V. S. Kaushik, J. Vac. Sci. Technol. B **18**, 2139 (2000).
[5]J. W. Reiner, A. Posadas, M. Wang, M. Sidorov, Z. Krivokapic, F. J. Walker, T. P. Ma, and C. H. Ahn, J. Appl. Phys. **105**, 124501 (2009).
[6]C. Merckling, G. Saint-Girons, C. Botella, G. Hollinger, M. Heyns, J. Dekoster, and M. Caymax, Appl. Phys. Lett. **98**, 092901 (2011).
[7]H. Seo, A. B. Posadas, C. Mitra, A. V. Kvit, J. Ramdani, and A. A. Demkov, Phys. Rev. B **86**, 075301 (2012).
[8]A. Posadas, M. Berg, H. Seo, D. J. Smith, H. Celio, A. P. Kirk, D. Zhernokletov, R. M. Wallace, A. de Lozanne, and A. A. Demkov, Appl. Phys. Lett. **98**, 053104 (2011) .
[9]C. Dubourdieu, J. Bruley, T. M. Arruda, A. Posadas, J. Jordan-Sweet, M. M. Frank, E. Cartier, D. J. Frank, S. V. Kalinin, A. A. Demkov, and V. Narayanan, Nat. Nanotechnol. **8**, 748 (2013).
[10]J. Y. Jo, Y. S. Kim, T. W. Noh, J.-G. Yoon, and T. K. Song, Appl. Phys. Lett. **89**, 232909 (2006).
[11]V. Vaithyanathan, J. Lettieri, W. Tian, A. Sharan, A. Vasudevarao, Y. L. Li, A. Kochhar, H. Ma, J. Levy, P. Zschack, J. C. Woicik, L. Q. Chen, V. Gopalan, and D. G. Schlom, J. Appl. Phys. **100**, 024108 (2006).
[12]S. Abel, T. Stöferle, C. Marchiori, C. Rossel, M. D. Rossell, R. Erni, D. Caimi, M. Sousa, A. Chelnokov, B. J. Offrein, and J. Fompeyrine, Nat. Commun. **4**, 1671 (2013).
[13]X. L. Li, H. B. Lu, M. Li, Z. Mai, H. Kim, and Q. J. Jia, Appl. Phys. Lett. **92**, 012902 (2008).
[14]F. Niu and B. W. Wessels, J. Vac. Sci. Technol. B **25**, 1053 (2007).
[15]G. Niu, S. Yin, G. Saint-Girons, B. Gautier, P. Lecoeur, V. Pillard, G. Hollinger, and B. Vilquin, Microelectron. Eng. **88**, 1232 (2011).
[16]M. Choi, A. Posadas, R. Dargis, C.-K. Shih, A. A. Demkov, D. H. Triyoso, N. D. Theodore, C. Dubourdieu, J. Bruley, and J. Jordan-Sweet, J. Appl. Phys. **111**, 064112 (2012).
[17]S. Abel, M. Sousa, C. Rossel, D. Caimi, M. D. Rossell, R. Erni, J. Fompeyrine, and C. Marchiori, Nanotechnology **24**, 285701 (2013).
[18]S. Salahuddin and S. Datta, Nano Lett. **8**, 405 (2008).
[19]A. I. Khan, D. Bhowmik, P. Yu, S. J. Kim, X. Pan, R. Ramesh, and S. Salahuddin, Appl. Phys. Lett. **99**, 113501 (2011).
[20]Z. Yu, J. Ramdani, J. A. Curless, J. M. Finder, C. D. Overgaard, R. Droopad, K. W. Eisenbeiser, J. A. Hallmark, W. J. Ooms, J. R. Conner, and V. S. Kaushik, J. Vac. Sci. Technol. B **18**, 1653 (2000).
[21]M. D. McDaniel, A. Posadas, T. Wang, A. A. Demkov, and J. G. Ekerdt, Thin Solid Films **520**, 6525 (2012).
[22]M. D. McDaniel, A. Posadas, T. Q. Ngo, A. Dhamdhere, D. J. Smith, A. A. Demkov, and J. G. Ekerdt, J. Vac. Sci. Technol. A **31**, 01A136 (2013).
[23]W. J. Merz, Phys. Rev. **95**, 690 (1954).
[24]R. A. Mckee, F. J. Walker, and M. F. Chisholm, Science **293**, 468 (2001).
[25]J. P. George, J. Beeckman, W. Woestenborghs, P. F. Smet, W. Bogaerts, and K. Neyts, Nanoscale Res. Lett. **8**(1), 62 (2013).
[26]P. R. Arya, P. Jha, G. N. Subbanna, and A. K. Ganguli, Mater. Res. Bull. **38**, 617 (2003).